XLIII CILAMCE
21–25, November, 2022
FOZ DO IGUAÇU – PR – BRAZIL

Non-linear numerical modeling of reinforced concrete structures considering bond slip

Adrielle N. Marques[1], Chiara P. Teodoro[1], Rogério Carrazedo[1]

[1]*Dept. of Structural Engineering, University of São Paulo at São Carlos School of Engineering*
Avenida Trabalhador são-carlense, 400, Zip-Code 13566-590, SP/São Carlos, Brazil
adriellenascimento@usp.br, chiarapteodoro@usp.br, rogcarrazedo@sc.usp.br

Abstract. Depending on the stress magnitude in the interface of rebar and concrete, relative displacements may develop. Thus, to develop a reliable numerical model, interaction between rebar and concrete must be included by a bond slip constitutive relationship. Therefore, in this work we propose a numerical model to evaluate the bond loss between reinforcement and concrete, based on the Positional Finite Element Method. In this method, geometric nonlinearities are considered and static equilibrium are obtained though the Principle of Stationary Potential Energy, considering total Lagrangian description. An incremental-iterative Newton-Raphson procedure was used to solve the non-linear system. Fibers (rebars) are immersed in the matrix (concrete) though nodal kinematic relationships, allowing mesh independency. Physical nonlinearity for concrete is considered by Mazars damage model, and for reinforcement it is considered an elastoplastic constitutive relationship. Bond rupture is simulated by Lagrange multipliers and relative displacement of matrix and fiber (slipping) is made up by a dimensionless bonding element after rupture. Results are compared to experimental and analytical examples, showing that the proposed method is reliable and accurate.

Keywords: Reinforced concrete; Adhesion loss; Bond slipping; Lagrange multipliers; Positional FEM.

1 Introduction

The bond between rebar and concrete in reinforced structures is the basic mechanics that allows transfer of forces between materials and restrain slipping. Usually, perfect bonding is considered and any relative displacement is neglected, thus neglecting the influence of interfacial transition zone (ITZ). Such simplification is accurate enough to simulate the global behavior of the structure and it is adequate to evaluate global safety in its useful life, as long as small displacements and rotations are considered. However, as structure is locally or globally overloaded, or as it undergoes any deterioration mechanisms, cracking and structural instabilities may develop, requiring an accurate description of the mechanical effects, including the loss of adhesion and bond slipping.

A useful life analysis without the loss of adhesion mechanism, will disregard the possibility of bond rupture. It is major drawback since this rupture is fragile, due to the following mechanics: crushing of concrete along rebar ribs, shearing of concrete around rebar, or, more frequently, longitudinal cracking of concrete cover along reinforcement (Barbosa and Sanchez Filho [1]). Thus, in order to attain a realistic analysis of reinforced concrete structures, one must include the interaction between reinforcement and concrete and the mechanism of stress transfer between these materials, therefore including failure modes associated to bond loss.

However, the mechanism of loss of adhesion is quite complex, and several uncertainties are involved for each constituent material and for the interaction between them. Steel can be considered homogeneous with well-defined properties, but concrete is heterogeneous. Besides, the reinforced concrete structure may present non-linear behavior depending on the stresses to which it is submitted, either from material non-linearities or geometric non-linearities (Marins Neto [2]).

The physical nonlinear behavior of the reinforced concrete is mainly due to cracking, shrinkage and creep, modifying the composite response and stress transfer between fiber and matrix depending on the deformation state. In a finite element analysis, physical non-linearities can be considered through complex constitutive relationships,

as there is no direct (linear) proportionality between stresses and strains depending on the applied load.

The geometric nonlinearity of a structure must be considered whenever moderate displacements take place. In this condition, equilibrium depends not only from on its initial geometry but also on the displacements themselves, leading to additional efforts.

When the finite element method is employed to model the bond slip, an additional difficulty arises to simulate the loss of adhesion – the connection of fiber and matrix are made though common nodes, which implies that no slipping may occur, imposing a compatibility condition of perfectly adherent materials. To consider slipping, connection elements are introduced to represent their interface and transmission of forces. These connection elements are governed by a constitutive law that establishes the non-linear relationship between the adhesion stress and slip based on experimental tests capable of describing the phenomenon.

We adopt an alternative version of the Finite Element Method, based on nodal positions instead of displacements, based on the work of Bonet et al. [3], Coda [4] and Coda [5]. Furthermore, the variational form is derived by the principle of stationary total mechanical energy, written in terms of current position, and the Saint-Venant-Kirchhoff kinematics is used in the compatibility equation – displacement/deformation relationship. An embedding technique is used to simulate composites, including reinforced concrete, whereas the reinforcement stiffness is immersed on the matrix elements considering that it adheres perfectly to the matrix (see, for instance, Paccola, Piedade Neto and Coda [6] and Paccola and Coda [7]).

In this work, we propose a technique that allows immersion of the reinforcement on the matrix but slipping may still take place. Concrete physical non-linearity is considered by Mazars damage model, and by an elastoplastic constitutive model for steel rebars. Bond slipping is simulated either by Lagrange multipliers and by dimensionless binding element that connect domains (matrix and fiber elements), following a limit state non-linear equation based on constitutive relationship at the interface. Some examples are included to validate the proposal.

2 Adhesion models

2.1 Reinforcement immersion

There are three ways to model the rebars in a finite element model of reinforced concrete (Simão [8], Hipólito et al. [9] and Wolenski et al. [10]) – distributed model, discrete model and embedded model, as seen in Figure 1.

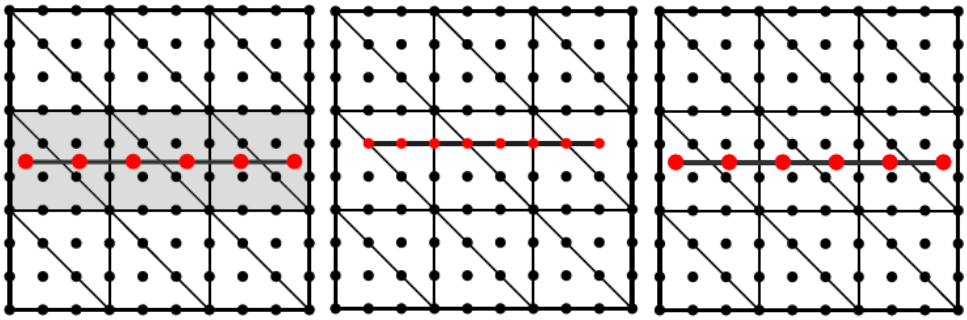

Figure 1. a) Distributed model; b) Discrete model; c) Embedded model

In the distributed model, the fiber stiffness is uniformly distributed on the matrix elements, thus properties are homogenized as a single material (Fig. 1a), sometimes even disregarding the fiber orientation (isotopically). This model is used when only global results are expected. Nevertheless, there is no way to model bond slipping in this case, as fiber elements are assimilated within the matrix properties.

In the discrete model, the fiber elements must be connected to the nodes of the matrix elements (Fig. 1b). Their stiffness are superimposed in the corresponding matrix degree of freedom. Notice that both domains (fiber and matrix) share the same node, thus the fiber displacement is conditioned to the matrix mesh geometry and displacement. One way to introduce bond slipping is to employ springs elements or continuous contact elements between matrix and reinforcement fibers, thus allowing relative displacements.

In embedded models, each fiber is considered as one-dimensional element immersed on the matrix, each with its own mesh (Fig. 1c). Fiber displacement are associated to the matrix by kinematic considerations, usually considering perfect adhesion between materials, thus no relative displacement is expected. To introduce slipping, extra nodes along the fiber elements are included, as in Balakrishna and Murray [11], Elwi and Hrudey [12], Allwood and Bajarwan [13] and Phillips and Wu [14], yet increasing the total number of degrees of freedom. Some authors also use fiber elements arbitrarily distributed in the matrix, but associate with the matrix mesh, as in discrete model, yet with their own nodes. For this reason, they often are classified as classify the model as semi-embedded, as in Durand [15], Rosero [16] and Durand and Farias [17].

In this work, we used the embedded model though kinematic relations between fiber and matrix (reinforcement bar and concrete), without increasing the total number of degrees of freedom while perfectly adherent. To describe the bond slip, new degrees of freedom are introduced by a dimensionless element, without modifying either the matrix or fiber meshes. Since these meshes are independent, this method allows to apply boundary conditions directly to the rebar elements, which makes it an effective way for the analysis of fiber pullout tests. Details of the Positional FEM and the embedded technique, applied to concrete, are seen in Ramos et al [18] and Ramos and Carrazedo [19].

2.2 Interaction between steel fiber and concrete matrix

With the reinforcement immersion technique already defined, an adequate representation of the interaction between rebar and concrete matrix is required. In this work, we used two mathematical elements – Lagrange multipliers and spring elements. The Lagrange multipliers are used to introduce kinematic constraints to the structural system, and are widely used in contact problems to prevent penetration of the materials. Here, we used to constrain the relative position of matrix node and reinforcement node, which connects domains. Once stress attains a critical value, the multipliers can be disabled, simulating a limit state for adherence. An advantage of using this method is that the value of the Lagrange multiplier is the force required to forbid slip, the adherence force, yet extra equations in the mathematical model for each Lagrange multiplier are imposed. Nevertheless, from the adherence force, the adhesion stress along rebar is calculated.

In our proposal, both meshes are independent (matrix and reinforcement), having their own nodes. A mirror node is immersed on the matrix – connect by kinematic relations – in the same coordinates than those from reinforcement fibers. These two nodes – fiber mesh and mirrored mesh – are connect by Langrage multipliers. In this way, the constraint is imposed and the adhesion force is obtained.

Since fiber node and mirrored mesh share the same coordinate, the distance between them is null, thus the constraint equation is given by:

$$\bar{Y}_i - \tilde{\phi}_j(\xi_1, \xi_2)\tilde{Y}_i^j = 0 \tag{1}$$

where $\bar{Y}$ are the current fiber nodal coordinates and $\tilde{Y}$ are the current coordinates of the matrix element in which the mirror node is immersed. The second term of equation (1) holds the coordinates of the mirror based on the dimensionless coordinates (ξ_1, ξ_2) and the shape function $\tilde{\phi}_j$ of the matrix element.

The total energy of the system (Π_L), considering the Lagrange multiplier, is defined by equation (2):

$$\Pi_L = U + P + \mathbb{L} \tag{2}$$

where U is the internal energy potential, P is the external energy potential, and $\mathbb{L}$ is the energy associated to the Lagrange multiplier. Since the Lagrange multiplier cannot change the total energy, it becomes a constraint equation. The energy functional associated to it is given by:

$$\mathbb{L} = \lambda_i \cdot \left[\bar{Y}_i - \tilde{\phi}_j(\xi_1, \xi_2)\tilde{Y}_i^j\right] \tag{3}$$

where λ_i are Lagrange multipliers associated to each direction.

The constraint equation adds new degrees of freedom to the numerical model, one equation for each Lagrange multiplier, even though the mirrored node is immersed on the matrix. The first derivative of the potential $\mathbb{L}$ with respect to the nodal parameters gives the contribution of the constraint equation to the internal forces, which is given by equations (4) to (6):

$$\frac{\partial \mathbb{L}}{\partial \bar{Y}_i} = \lambda_i \tag{4}$$

$$\frac{\partial \mathbb{L}}{\partial \bar{Y}_i} = -\lambda_i \tag{5}$$

$$\frac{\partial \mathbb{L}}{\partial \lambda_i} = \bar{Y}_i - \tilde{\phi}_j(\xi_1, \xi_2)\tilde{Y}_i^j \tag{6}$$

The second derivative of the potential $\mathbb{L}$ with respect to the nodal parameters gives the contribution of the constraint equation to the Hessian matrix:

$$\frac{\partial^2 \mathbb{L}}{\partial \bar{Y}_i \partial \bar{Y}_l} = \frac{\partial^2 \mathbb{L}}{\partial \tilde{Y}_i \, \partial \tilde{Y}_l} = \frac{\partial^2 \mathbb{L}}{\partial \bar{Y}_i \partial \tilde{Y}_l} = \frac{\partial^2 \mathbb{L}}{\partial \tilde{Y}_i \, \partial \bar{Y}_l} = 0 \tag{7}$$

$$\frac{\partial^2 \mathbb{L}}{\partial \bar{Y}_i \, \partial \lambda_l} = \frac{\partial^2 \mathbb{L}}{\partial \lambda_i \, \partial \bar{Y}_l} = 1 \tag{8}$$

$$\frac{\partial^2 \mathbb{L}}{\partial \tilde{Y}_i \, \partial \lambda_l} = \frac{\partial^2 \mathbb{L}}{\partial \lambda_i \, \partial \tilde{Y}_l} = -1 \tag{9}$$

The Lagrange multiplier has the value, in the equilibrium situation of the structure, of the contact force necessary to forbid relative displacement, from which the bond stress can be easily calculated.

The second way to represent the interaction between rebar and concrete matrix, as mentioned before, is to employ springs. These have the advantage of not introducing new variables, as seen in Lagrange multiplier, and they may behave non-linearly. As before, two independent meshes with their own nodes are connect but here by dimensionless springs. The restraining equation, imposed by the spring, is given by the following potential:

$$\mathbb{M} = \frac{k}{2}\left[\bar{Y}_i - \tilde{\phi}_j(\xi_1, \xi_2)\tilde{Y}_i^j\right]^2 \tag{10}$$

in which k is the spring stiffness.

The first derivative of the potential $\mathbb{M}$ with respect to the nodal parameters gives the contribution of the constraint equation to the internal forces, which is given by equations (11) and (12). These are the contact forces between fiber and matrix, the adhesion force.

$$\frac{\partial \mathbb{M}}{\partial \bar{Y}_i} = k \cdot \left[\bar{Y}_i - \tilde{\phi}_j(\xi_1, \xi_2)\tilde{Y}_i^j\right] \tag{11}$$

$$\frac{\partial \mathbb{M}}{\partial \tilde{Y}_i} = -k \cdot \left[\bar{Y}_i - \tilde{\phi}_j(\xi_1, \xi_2)\tilde{Y}_i^j\right] \tag{12}$$

The second derivative of the potential $\mathbb{M}$ with respect to the nodal parameters gives the contribution of the constraint equation to the Hessian matrix:

$$\frac{\partial^2 \mathbb{M}}{\partial \bar{Y}_i \partial \bar{Y}_l} = \frac{\partial^2 \mathbb{M}}{\partial \tilde{Y}_i \, \partial \tilde{Y}_l} = \; k \tag{13}$$

$$\frac{\partial^2 \mathbb{M}}{\partial \bar{Y}_i \partial \tilde{Y}_l} = \frac{\partial^2 \mathbb{M}}{\partial \tilde{Y}_i \, \partial \bar{Y}_l} = \; -k \tag{14}$$

In our proposal, the Lagrange multiplier allows to stablish the limit state for adherence. Once it is attained, the Lagrange multiplier is disabled. On the other hand, the spring element evaluates the bond-slip behavior. In either way, the value obtained are the contact forces, associated to the matrix element direction. To evaluate the shear and normal stress to the fiber element, the contact forces are rotated to the tangential and normal directions, as given by equation (15):

$$\begin{Bmatrix} Q \\ P \end{Bmatrix} = \begin{bmatrix} cos\ \alpha & sen\ \alpha \\ sen\ \alpha & cos\ \alpha \end{bmatrix} \cdot \begin{Bmatrix} F_{c1} \\ F_{c2} \end{Bmatrix} \tag{15}$$

where α is fiber element orientation angle, and Q and P are the contact forces components in the tangential and normal direction, respectively. If node is common to two elements, the contact force is given by the average value. These forces are divided by the influence surface, resulting in shear (τ_m) and normal (σ_m) stresses along the interface, according to equations (16) and (17), respectively:

$$\tau_m = \frac{Q}{A_{inf}} = \frac{Q}{p \cdot c_{inf}} \tag{16}$$

$$\sigma_m = \frac{P}{A_{inf}} = \frac{P}{p \cdot c_{inf}} \tag{17}$$

where p is the fiber perimeter and c_{inf} is the node influence distance.

2.3 Physical non-linearity

The complexity involved in the study of concrete is one of the great challenges for a complete description of adhesion problems, due to several factors such as: physical non-linearity at low stress levels; the difference in tensile and compressive strengths; creep and shrinkage; and cracking and transmission of stresses through cracks (Bono [20]). Based on the theory of plasticity, elasticity, and fracture and damage mechanics, several studies were developed to model the behavior of concrete. Among them, the damage model proposed by Mazars [21] is widespread and, although isotropic, it able to represent concrete damage.

The Mazars damage model is based on a scalar damage variable that reduces concrete stiffness when positive strain exceeds a reference value. The scalar damage variable is obtained by a linear combination between a tension and a compression portion, so that 1 represents a state of total degradation at the point, while 0 means that the material is completely intact. The following hypothesis are adopted by the model: damage is caused by positive strains; concrete is elastic all the way; loading is monotonous increasing, that is, no residual deformation is considered after unloading; damage is isotropic.

For rebar, an elastoplastic model with isotropic linear hardening was adopted. The stress-strain relationship is characterized by an initial elastic stretch followed by a yield point with work hardening. In this point, there may be an intense reduction in the stiffness of the material. The longitudinal modulus of elasticity, the yield stress and the plastic modulus of isotropic hardening are the parameters for characterization of the material.

3 Examples

Three numerical examples to verify the formulations presented, in order to evaluate accuracy, practicality and efficiency. Experimental and numerical results were used in the validation examples.

3.1 Example 1 - Column with eccentric load and geometric imperfection

In this first example, a non-linear physical and geometrical reinforced concrete column is subjected to an eccentric load, considering rebar and concrete perfectly adherent using the embedded technique, to validate the numerical model. According to Bratina et al. [22], this is a widespread example in the literature for validating numerical models of reinforced concrete, called Foure's column. The results obtained will be compared with the experimental test documented by Espion [23] and other authors computational models, such as Liu et al. [24], Parente et al. [25] and Ramos [26].

The geometric properties, static scheme and loading conditions used in the example are shown in Figure 3, in which an initial imperfection of 0.1% of the length of the element (h) is also adopted. The properties of the concrete and steel are, respectively: modulus of elasticity, E_c = 3,360 kN/cm² and E_s = 21,000 kN/cm²; Poisson's ratio, ν_c = 0,20 e ν_s = 0,00; and steel yield stress, considering the perfect elastoplastic behavior, f_y = 46.5 kN/cm². Besides, following Ramos [26], the adopted parameters for Mazars Damage model were: ε_{d0} = 0.0000865, A_t = 0.50, B_t = 9,000, A_c = 1.20 e B_c = 1,500.

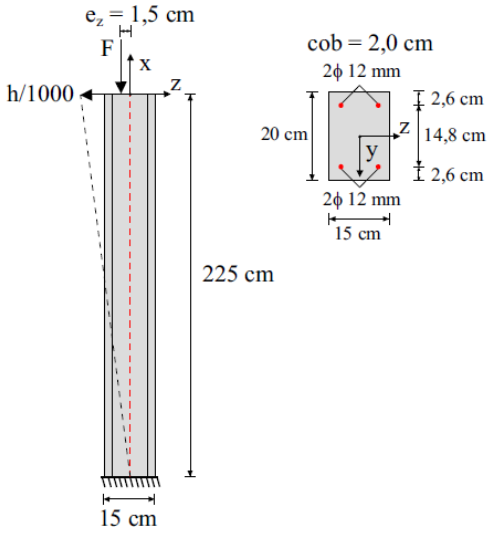

Figure 3. Geometric properties for Foure's column. Source: Ramos [26].

The column was discretized with 960 triangular elements of cubic order and the reinforcement with 900 linear elements, resulting in 10,890 degrees of freedom. Displacement control was used, applying a vertical displacement of 0.6 cm divided into 50 steps, in the position of F. Thus, the vertical force F was measured and shown in Figure 4. The maximum load supported by the column was 447.78 kN, a deviation of 0.54% from the experimental result. The accuracy shown in Figure 4 indicates that the model can be used to evaluate concrete elements under axial and bending loading conditions.

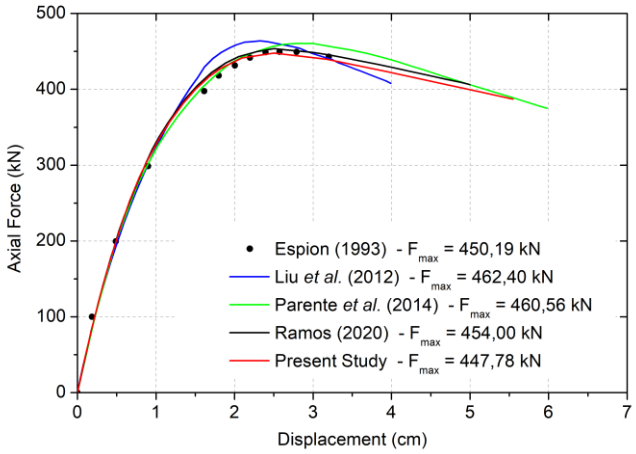

Figure 4. Force vs displacement for Foure's column.

3.2 Example 2 - Bar with stiffeners

In this example, a rectangular bar with four rebars is subject to displacements at both ends, as shown in Figure 5. Results are compared to Sampaio [27], using a linear model to validate the Lagrange multipliers in the connection between matrix and fibers, using the immersed technique.

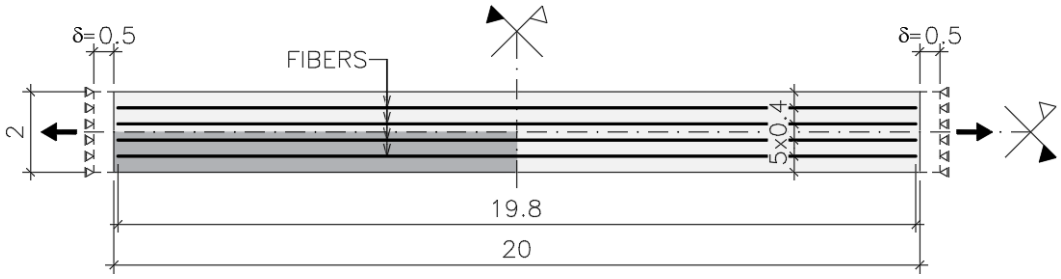

Figure 5. Reinforced beam under prescribed displacement at both ends.

Beam cross section is given by 1 x 2 cm, and rebar of 0.01 cm². The following properties are adopted: Young modulus E_{fiber} = 100.000 kN/cm² and E_{matrix} = 2.000 kN/cm²; Poisson's ratio $\nu_{fiber} = \nu_{matrix}$ = 0,0. A displacement of $0.5.10^{-4}$ is imposed at both ends. Only one quarter of the beam was modeled, using 864 triangular elements of cubic approximation for matrix and 240 linear elements to discretize the fibers, resulting in 8,730 degrees of freedom. The mesh refinement is shown in Figure 6.

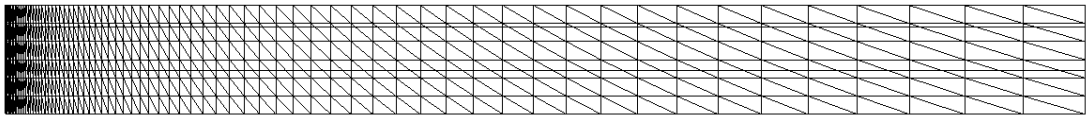

Figure 6. Mesh discretization with greater refinement at the beam end

Sampaio [27] calculated the interface stresses by decomposing the internal force of the fiber into normal and tangential force. In our case, since Lagrange multipliers were used to connect domains, the contact forces are readily obtained. Even though reference [27] used cubic elements to discretize the fibers, results are quite close, as seen in Figure 7.

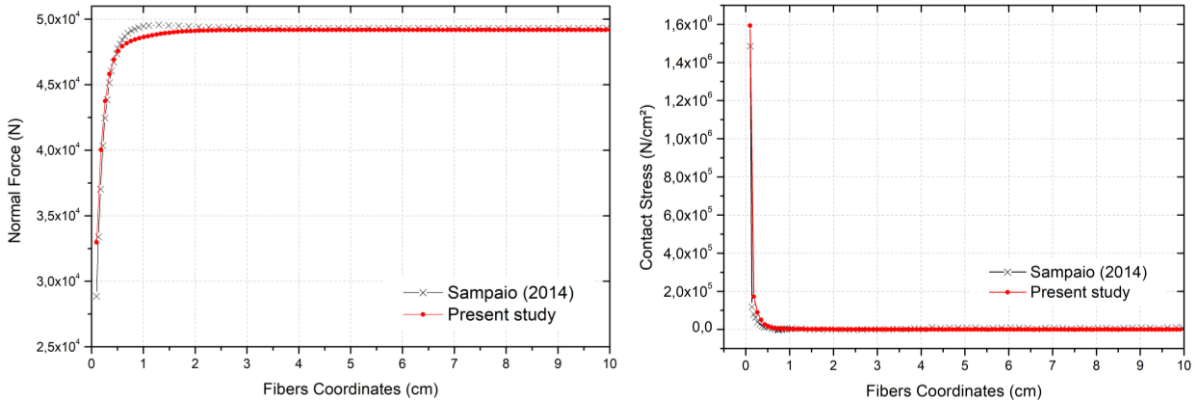

Figure 7. Normal force and contact stress with fully adherent model.

A second analysis was made in which we imposed a limit value of 15,000 N/cm² for the contact stress, disconnecting nodes that achieved this value. Free slip will then occur for those nodes, and force should be transferred to other elements. This behavior was correctly obtained, as seen in Figure 8.

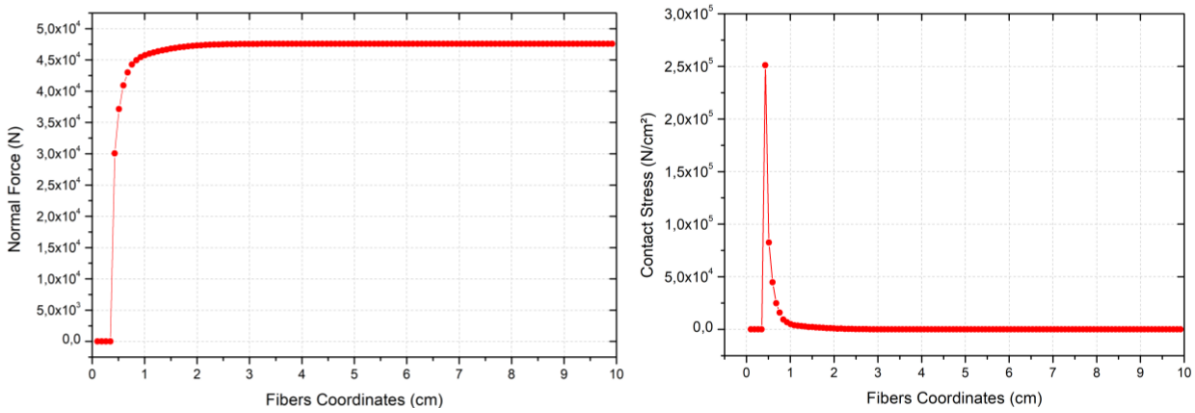

Figure 8. Normal force and contact stress with fiber slip model.

3.3 Example 3 – Pull out

A pull-out test is modeled as third example. Spring elements were inserted to connect fiber and matrix elements, allowing relative displacements between domains. Paccola, Piedade Neto and Coda [6] proposed this example, as seen in Figure 9, considering elastic matrix and fiber, with: E_{fiber} = 200,000 kN/mm² and E_{matrix} = 20,000 kN/mm²; ν_{matrix} = 0.2; $e_{matrix} = e_{fiber}$ = 1 mm; and A_{fiber} = 0.1 mm². Perfectly elastoplastic contact is assumed, with k = 1000 kN/mm² and τ_y = 51.6 kN/mm². A single force was applied directly to the rebar, until limit of 849.51 kN is achieved.

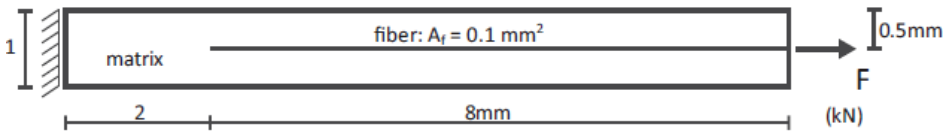

Figure 9. Geometry for pull out test. Source: Paccola, Piedade Neto and Coda [6].

A uniform mesh of 320 triangular element with cubic approximation and 160 linear elements with linear approximation was used to discretize the problem, resulting in 3,468 degrees of freedom. Figure 10 shows the mesh and the deformed configuration when F = 849.51 kN – the maximum load that we were able to use, which deviates 1.96% from the force found in the reference [6].

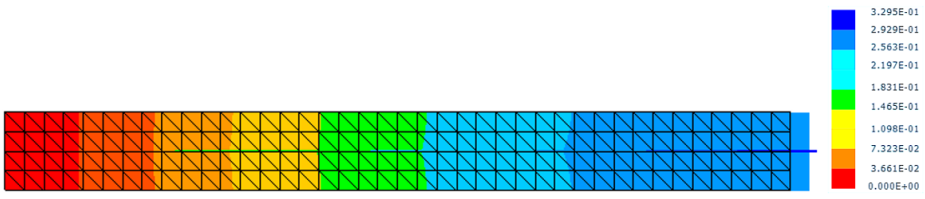

Figure 10. Deformed configuration for F = 849.51 kN.

As the rebar is pulled, it is expected that the contact shear stresses at ends to be maximum and descending to the center. As the fiber slips, stresses at center increases until complete failure. Figure 11a shows the contact shear stresses with increasing force, with the expected behavior. In Figure 11b, it is shown the normal stresses, which tends to increase and becomes linearly distributed as bond slipping develops. Results are compared to reference [6], showing good agreement, indicating that the proposed technique was able to represent the non-linear behavior of bond slip.

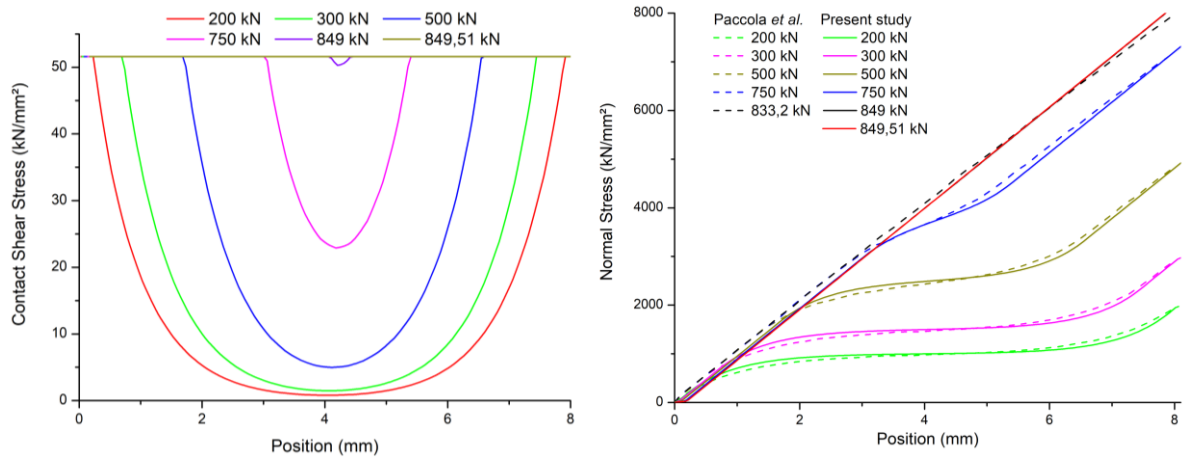

Figure 11. Bond stresses along fiber. (a) Shear stresses; (b) Normal stresses.

4 Conclusions

The numerical model presented in this article includes two different approaches to consider the loss of bond in reinforced structures, one using Lagrange multipliers and the other using spring elements. To allow the reinforcement to be inserted into the matrix independently, the embedding method was used. Due to the high stiffness of the connection with the use of Lagrange multipliers, this approach is more suitable for low shear stresses at the interface, where the fiber slip is not very expressive, as in the calculation of the bond length of reinforced concrete elements. For high shear stresses at the interface, as in fiber pullout tests, the use of spring elements is more recommended because it represents the degradation of the interface through the decrease in spring stiffness, which allows the fiber to slip. The formulations presented were validated with experimental and numerical results from several authors. Thus, it is assumed that the numerical model presented can be applied for a more realistic analysis of reinforced concrete structures, considering the physical, geometric and contact non-linearities inherent to the system.

Acknowledgements. The research supported by the Brazilian National Council for Scientific and Technological Development is gratefully acknowledged. This study was also financed in part by the Coordenação de Aperfeiçoamento de Pessoal de Nível Superior - Brasil (CAPES) - Finance Code 001.

Authorship statement. The authors hereby confirm that they are the sole liable persons responsible for the authorship of this work, and that all material that has been herein included as part of the present paper is either the property (and authorship) of the authors, or has the permission of the owners to be included here.

References

[1] M. T. G. Barbosa and E. S. Sanchez Filho, "The bond stress x slipping relationship," *Revista IBRACON de Estruturas e Materiais*, vol. 9, nº 5, pp. 745-753, 2016.

[2] J. Marins Neto, "Analise numerica não-linear de estruturas de concreto armado considerando o fenômeno da aderência entre o aço e o concreto," Tese (Doutorado em Engenharia Civil) — Faculdade de Engenharia Civil, Arquitetura e Urbanismo, Universidade Estadual de Campinas, Campinas, 2007.

[3] J. Bonet, R. D. Wood, J. Mahaney and P. Heywood, "Finite element analysis of air supported membrane structures," *Computer Methods in Applied Mechanics and Engineering*, vol. 190, nº 5-7, pp. 579-595, 2000.

[4] H. B. Coda, "An exact fem geometric non-linear analysis of frames based on position description," In.: 17th International Congress of Mechanical Engineering, São Paulo, 2003.

[5] H. B. Coda, O método dos elementos finitos posicional: sólidos e estruturas - não linearidade geométrica e dinâmica, São Carlos: EESC-USP, 2018, p. 284.

[6] R. R. Paccola, D. Piedade Neto e H. B. Coda, "Geometrical non-linear analysis of fiber reinforced elastic solids considering debounding," *Composite Structures,* vol. 133, pp. 343-357, 2015.

[7] R. R. Paccola and H. B. Coda, "A direct FEM approach for particulate reinforced elastic solids," *Composite Structures,* vol. 141, pp. 282-291, 2016.

[8] W. I. S. Simao, "Modelos de armadura e aderência para análise não-linear de estruturas de concreto armado," Dissertação (Mestrado em Estruturas) - Escola de Engenharia, Departamento de Engenharia de Estruturas, Universidade Federal de Minas Gerais, Belo Horizonte, 2003.

[9] F. Hipólito, R. Durand and E. Pains, "Aplicação de elementos de junta na análise de estruturas de concreto armado," *Revista Interdisciplinar de Pesquisa em Engenharia,* vol. 2, nº 23, pp. 145-164, 2017.

[10] A. R. V. Wolenski, S. S. Castro, A. B. Monteiro, S. S. Penna and R. Pitangueira, "Modelos constitutivos de microplanos e perda de aderência na análise de estruturas de concreto armado," In.: 56º Congresso Brasileiro do Concreto, Natal, 2014.

[11] S. Balakrishna and D. Murray, "Prediction of response of concrete beams and panels by nonlinear finite element analysis," *IABSE Reports,* pp. 393-404, 1987.

[12] A. E. Elwi and T. M. Hrudey, "Finite element model for curved embedded reinforcement," *Journal of Engineering Mechanics,* vol. 115, nº 4, pp. 740-754, 1989.

[13] R. J. Allwood and A. A. Bajarwan, "A new method for modelling reinforcement and bond in finite element analyses of reinforced concrete," *International Journal for Numerical Methods in Engineering,* vol. 28, nº 4, pp. 833-844, 1989.

[14] D. V. Philips and Z. P. Wu, "An oriented bar formulation with bond-slip," In: Proceeding of the international conference on numerical method in engineering: Theory and application, 1990.

[15] R. D. Durand, "Análise tridimensional de estruturas geotécnicas submetidas a reforço e drenagem," Tese (Doutorado em Geotecnia)—Universidade de Brasília, Brasília, 2008.

[16] B. G. P. Rosero, "Análise dinâmica de estruturas de concreto armado via elementos finitos," Dissertação (Mestrado em Estruturas e Construção Civil)—Universidade de Brasília, Brasília, 2018.

[17] R. D. Durand and M. M. Farias, "Nonlinear Joint Element for the Analysis of Reinforcement," *10th World Congress on Computational Mechanics,* vol. 1, pp. 3253-3268, 2014.

[18] E. S. Ramos, R. Carrazedo and R. R. Paccola, "Modeling particle elements in damaged reinforced concrete structures", *Latin American Journal of Solids and Structures,* vol. 18, nº 1, 2021.

[19] E. S. Ramos and R. Carrazedo, "Numerical analysis of reinforced concrete beam subject to pitting corrosion", *Ambiente Construído,* vol. 22, pp. 201-222, 2022.

[20] G. F. F. Bono, "Modelos constitutivos para análise tridimensional de estruturas de concreto armado através do método dos elementos finitos," Tese (Doutorado em Engenharia Civil) - Universidade Federal do Rio Grande do Sul, Porto Alegre, 2008.

[21] J. Mazars, "Application de la mécanique de l'endommagement au comportement non linéaire et à la rupture du béton de structure," Tese (Docteur es Sciences) — Universite Pierre et Marie Curie, Paris, 1984.

[22] S. Bratina, M. Saje and I. Planinc, "On material and geometrically non-linear analysis of reinforced concrete planar frames," *International Journal of Solids and Structures,* vol. 41, nº 24, pp. 7181-7207, 2004.

[23] B. Espion, "Benchmark examples for creep and shrinkage analysis computer programs," In.: Proc. 5th Int. RILEM Symposium on Creep and Shrinkage of Concrete, Barcelona, 1993.

[24] S.-W. Liu, Y.-P. Liu and S.-L. Chan, "Advanced analysis of hybrid steel and concrete frames: Part 2: Refined plastic hinge and advanced analysis," *Journal of Constructional Steel Research,* vol. 70, pp. 337-349, 2012.

[25] E. Parente Junior, G. V. Nogueira, M. Meireles Neto and L. S. Moreira, "Material and geometric nonlinear analysis of reinforced concrete frames," *Rev. IBRACON Estrut. Mater.,* vol. 7, nº 5, pp. 879-904, 2014.

[26] É. S. Ramos, "Modelagem numérica da propagação da corrosão por cloretos em estruturas de concreto armado," Dissertação (Mestrado em Estruturas) - Departamento de Engenharia de Estruturas, EESC - USP, São Carlos, 2020.

[27] M. S. M. Sampaio, "Análise não linear geométrica de cascas laminadas reforçadas com fibras," Tese (Dourado) - Departamento de Engenharia de Estruturas - EESC-USP, São Carlos, 2014.